

# The variation of integrated star IMFs among galaxies

C. Weidner and P. Kroupa

*Sternwarte der Universität Bonn, 53121 Bonn, Germany*

cweidner@astro.uni-bonn.de

pavel@astro.uni-bonn.de

## ABSTRACT

The integrated galaxial initial mass function (IGIMF) is the relevant distribution function containing the information on the distribution of stellar remnants, the number of supernovae and the chemical enrichment history of a galaxy. Since most stars form in embedded star clusters with different masses the IGIMF becomes an integral of the assumed (universal or invariant) stellar IMF over the embedded star-cluster mass function (ECMF). For a range of reasonable assumptions about the IMF and the ECMF we find the IGIMF to be steeper (containing fewer massive stars per star) than the stellar IMF, but below a few  $M_{\odot}$  it is invariant and identical to the stellar IMF for all galaxies. However, the steepening sensitively depends on the form of the ECMF in the low-mass regime. Furthermore, observations indicate a relation between the star formation rate of a galaxy and the most massive young stellar cluster in it. The assumption that this cluster mass marks the upper end of a young-cluster mass function leads to a connection of the star formation rate and the slope of the IGIMF above a few  $M_{\odot}$ . The IGIMF varies with the star formation history of a galaxy. Notably, large variations of the IGIMF are evident for dE, dIrr and LSB galaxies with a small to modest stellar mass. We find that for any galaxy the number of supernovae per star (NSNS) is suppressed relative to that expected for a Salpeter IMF. Dwarf galaxies have a smaller NSNS compared to massive galaxies. For dwarf galaxies the NSNS varies substantially depending on the galaxy assembly history and the assumptions made about the low-mass end of the ECMF. The findings presented here may be of some consequence for the cosmological evolution of the number of supernovae per low-mass star and the chemical enrichment of galaxies of different mass.

*Subject headings:* galaxies: abundances – galaxies: evolution – galaxies: general – galaxies: star clusters – galaxies: stellar content – galaxies: structure

## 1. Introduction

Over the last years it became clear that star formation takes place mostly in embedded clusters, each cluster containing a dozen to many million stars (Kroupa 2004). Within these clusters stars appear to form following a universal initial mass function (IMF) with a Salpeter power-law slope or index ( $\alpha = 2.35$ ) for stars more massive than  $1 M_{\odot}$ ,  $\xi(m) \propto m^{-\alpha}$ , where  $\xi dm$  is the number of stars in the mass interval  $m, m + dm$ .

This has been found to be the case for a wide range of different conditions in the Milky Way (MW), the Large and Small Magellanic clouds (respectively LMC, SMC) and other galaxies (Massey & Hunter 1998; Sirianni et al. 2000, 2002; Parker et al. 2001; Massey 2002, 2003; Wyse et al. 2002; Bell et al. 2003; Piskunov et al. 2004). For studies based on well-resolved stellar populations, the observational scatter around the Salpeter value above  $1M_{\odot}$  is large but constant as a function of stellar mass range and consistent with a Gaussian distribution around this value (Fig. 1). This scatter can be explained by statistical fluctuations and stellar-dynamical evolution of the clusters (Elmegreen 1999; Kroupa 2001). The latter changes the mass function on short and long timescales - making it extremely difficult to measure the IMF. Careful studies taking mass segregation into account often find Salpeter indices in young clusters (e.g. in the LMC and SMC, Gouliermis et al. 2004a). Furthermore a Salpeter IMF is found in very young clusters such as the star-burst cluster R136 in the LMC (Brandl et al. 1996), NGC 1805 (de Grijs et al. 2002), NGC 2004, NGC 2100 (Gouliermis et al. 2004a) and M82-F (McCraday et al. 2004). The often-observed flattening of the IMF below a few solar masses (e.g. Sirianni et al. 2000) can be explained by taking mass segregation into account (Sirianni et al. 2002; de Marchi et al. 2004). Especially fig. 2 from Massey (2003) demonstrates the remarkable universality of the IMF over a factor of 4 in metallicity and 200 in stellar density.

On the other hand, several observations (e.g. Prisinzano et al. 2001, 2003; Sagar et al. 2001; Sanner & Geffert 2001; Kalirai et al. 2003) show steeper slopes for clusters with ages of 100 - 500 Myr and for stars ranging up to 4 - 15  $M_{\odot}$ . For the Pleiades cluster which has an age of about 100 Myr, Moraux et al. (2004) find the IMF may be steeper than Salpeter ( $\alpha > 2.35$ ) for  $m \gtrsim 2 M_{\odot}$ . While these are important constrains, it is clear that such clusters are already heavily dynamically evolved (Kroupa et al. 2001). Gualandris et al. (2004) show for the very young Trapezium cluster that two OB-run-away stars as far away as about 250 pc can be traced back to it. Furthermore, about 40% of O stars and 5-10% of B stars are run-away stars most probably ejected from star-forming regions (Gualandris et al. 2004) and found up to several kpc away from their birth places. Obviously such stars need to be included in order to reconstruct an IMF from a present-day mass function (PDMF) which has not been done. But also stars 'evaporating' from a cluster after gas expulsion

would travel 100 to 500 pc for clusters that are 100 to 500 Myr old even if they leave only with a velocity of  $1 \text{ km s}^{-1}$ ! Thus, dynamical modelling on a cluster-to-cluster basis would be needed to affirm possible non-Salpeter IMFs above  $1 M_{\odot}$ .

So the case may be made that the IMF differs from cluster to cluster (Scalo 1998, 2004; Elmegreen 2004a). However, the absence of any trends with physical conditions together with the Gaussian distribution about the Salpeter value above  $\sim 1 M_{\odot}$  and the similar, although somewhat larger theoretical spread obtained for model clusters (Fig. 1), leads us to assume for now that the stellar IMF is invariant and universal in each cluster. In addition to using our default canonical Salpeter IMF above  $1 M_{\odot}$ , we also construct models with  $\alpha = 2.70$  to account for a possibly steeper-than-Salpeter universal IMF above  $1 M_{\odot}$ .

Several studies show that star clusters also seem to be distributed according to a power-law embedded cluster mass function (ECMF),  $\xi_{\text{ecl}} = k_{\text{ecl}} M_{\text{ecl}}^{-\beta}$ , where  $dN_{\text{ecl}} = \xi_{\text{ecl}}(M_{\text{ecl}}) dM_{\text{ecl}}$  is the number of embedded clusters in the mass interval  $M_{\text{ecl}}, M_{\text{ecl}} + dM_{\text{ecl}}$  and  $M_{\text{ecl}}$  is the mass in stars. For embedded stellar clusters in the solar neighborhood with masses between 50 and  $1000 M_{\odot}$ , Lada & Lada (2003) find a slope  $\beta = 2$ , while Hunter et al. (2003) find  $2 \lesssim \beta \lesssim 2.4$  for  $10^3 \lesssim M_{\text{ecl}}/M_{\odot} \lesssim 10^4$  in the SMC and LMC, and Zhang & Fall (1999) find  $1.95 \pm 0.03$  for  $10^4 \lesssim M_{\text{ecl}}/M_{\odot} \lesssim 10^6$  in the Antennae galaxies. Our default assumption is a single-slope power-law ECMF with a lower limit of  $5 M_{\odot}$ , but different assumptions in the low cluster-mass regime are investigated as well.

Below roughly 100 stars ( $\sim 30 M_{\odot}$ ) embedded clusters dissolve within a few Myr (Adams & Myers 2001; Kroupa & Bouvier 2003) but for our model only the initial distribution of  $M_{\text{ecl}}$  is of interest, not the evolution of the clusters. The detailed distribution of such small systems is not well known. Observational and theoretical evidence is contradictory as Soares et al. (2004) conclude that they are not major contributors to the field, while Adams & Myers (2001) suggest that 90% of star-formation takes place in such small systems. This would be roughly equivalent to a power-law function with  $\beta \sim 2.35$  down to about  $5 M_{\odot}$  which corresponds to a group of about 20 stars. From a careful study of 580 open clusters in the Milky Way de la Fuente Marcos & de la Fuente Marcos (2004) find that 90% of the open clusters are formed with less than 150 stars. They are able to fit a power-law cluster mass function as steep as  $\beta = 2.7$  to the distribution down to a cluster mass of a few solar masses. 65% of the clusters in their sample have reconstructed masses less than  $20 M_{\odot}$ . They also conclude that 80% of newly formed open clusters will dissolve in less than 20 Myr.

A universality of the ECMF slope is not an established result as a number of works based on HII-region luminosity functions (Kennicutt et al. 1989; Youngblood & Hunter 1999; Alonso-Herrero et al. 2002; Thilker et al. 2002), direct cluster counts (Cresci et al. 2004) and GMC counts (Blitz & Rosolowski 2004) indicate that it may vary with galaxy-type or even

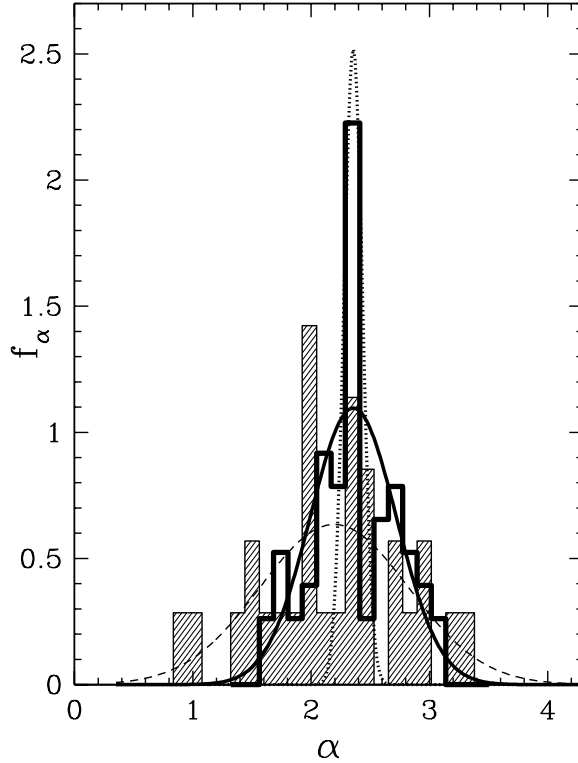


Fig. 1.— The thick solid histogram shows the observed MF power-law indices  $\alpha$  above  $2.5 M_{\odot}$  for an ensemble of clusters and associations in the MW, the LMC and SMC. Note the symmetry and narrowness of the empirical data that comprise a compilation of many OB populations in different physical systems. Note also that IMFs with  $\alpha < 1.6$  are never observed. Such IMFs would unbind a young cluster rapidly due to stellar evolutionary mass-loss (Kroupa 2001). The shaded histogram shows theoretical data: 12 star clusters with 800 to  $10^4$  stars are set-up with the canonical IMF (§ 2.2) and their slopes,  $\alpha$ , are evaluated after 3 and 70 Myr of dynamical and stellar evolution. Binaries are merged to give the system MFs which are used to measure  $\alpha$ . The models give an even greater spread than the observations although they assume a single (Salpeter) value for stars more massive than  $0.5 M_{\odot}$ ! Also shown are Gaussian distributions with standard deviations,  $\sigma_{\alpha}$ , obtained from the histograms. The thick solid line is for the observations and the dashed for the models. The very narrow dotted line is the Gaussian distribution for a fixed  $\alpha_f = \langle \alpha \rangle = 2.36$  and using only  $|\alpha| \leq 2\sigma_{\alpha}$ ,  $\sigma_{\alpha} = 0.63$ . For more details see Kroupa (2002).

rather erratically. The situation may be resolved once early cluster evolution is taken into account in more detail; Kroupa & Boily (2002) have already made the important point that the cluster MF evolves rapidly within the first few  $10^6$  yr as a result of re-virialisation after significant residual-gas expulsion.

Under the assumption that (i) the stellar IMF is universal and canonical and (ii) that the ECMF is also universal, we showed in Kroupa & Weidner (2003) that the integrated galaxial initial stellar mass function (IGIMF) must be steeper than the individual canonical IMFs in the actual clusters. But this steepening is critically dependent on the assumptions regarding the low-mass end of the ECMF.

In this contribution we develop a tool to calculate the time-dependent IGIMF for different types of galaxies. This is possible by combining the above mentioned results with a recently discovered relation between the maximum cluster mass formed in a star-formation epoch and the star formation rate (SFR) of a galaxy (Weidner et al. 2004). The varying star formation histories (SFHs) of galaxies therefore leave their fingerprint in the distribution of the stellar content and the resulting chemical evolution of galaxies through a highly variable IMF. However, this ought to be difficult to observe because variations of the SFR also imply changes of the relative number of young and old stars, even for an invariant IGIMF.

In the next section (§2) we introduce the method of calculating the IGIMF from a universal IMF, an ECMF and a star formation history (SFH), before we present the results in §3, where we construct standard, maximal and minimal models that span the range of parameters characterizing the stellar IMF and the ECMF. The results are discussed in §4. Before proceeding we note that throughout this paper IMF means the stellar IMF which we take to be invariant.

## 2. The method

### 2.1. The star-formation-rate–maximal-cluster-mass-relation

In Weidner et al. (2004) we derived a relation between the maximal cluster mass in a galaxy and the current star formation rate (SFR) of the galaxy,

$$\log_{10}(M_{\text{ecl,max}}) = \log_{10}(k_{\text{ML}}) + (0.75(\pm 0.03) \cdot \log_{10} SFR) + 6.77(\pm 0.02), \quad (1)$$

where  $k_{\text{ML}}$  is the mass-to-light ratio, typically 0.0144 for young ( $< 6$  Myr) clusters. This relation connects the properties of clustered star formation with the SFR of a galaxy. Of interest for investigating the sensitivity of the results on the SFR is also the use of a relation which is steeper than the default eq. 1 but still within the three-sigma uncertainty range of

the data,

$$\log_{10}(M_{\text{ecl,max}}) = \log_{10}(k_{\text{ML}}) + (0.84 \cdot \log_{10} SFR) + 6.71. \quad (2)$$

For a given SFR this relation gives larger  $M_{\text{ecl,max}}$  values than eq. 1.

Weidner et al. (2004) show that eq. 1 can be reproduced theoretically for a power-law ECMF provided the entire population of star clusters with masses ranging from  $M_{\text{ecl,min}} \approx 5 M_{\odot}$  to  $M_{\text{ecl,max}}$  is born within a time-span of  $\delta t \approx 10$  Myr, independently of the SFR. We refer to this time-span as a “star-formation epoch” of a galaxy. As these epochs are very short and the clusters fade quickly, a constant  $k_{\text{ML}}$  can be chosen and the ECMF and the resulting IGIMF can be determined within each epoch. We note that we differentiate between an embedded cluster that contains the entire stellar population formed in one molecular cloud core, while on the other hand the “initial cluster MF” has been introduced as a theoretical construct arrived at by mapping present-day cluster masses backwards in time using classical N-body evolution tracks that do not take into account violent virialisation owing to gas expulsion (Kroupa & Boily 2002). Thus, de la Fuente Marcos & de la Fuente Marcos (2004) derive an initial cluster MF in the local MW disk with a steeper slope ( $\beta \approx 2.7$ ) than  $\beta \approx 2$  suggested by local surveys of very young embedded clusters (Lada & Lada 2003). The de la Fuente initial cluster MF is likely to be biased towards smaller masses.

## 2.2. The canonical IMF and the maximal stellar mass in a cluster

The universal or canonical stellar IMF is conveniently written (Kroupa 2001; Reid et al. 2002) as a multi-power-law,  $\xi(m) \propto m^{-\alpha_i}$ , with exponents  $\alpha_0 = +0.30$  ( $0.01 \leq m/M_{\odot} < 0.08$ ),  $\alpha_1 = +1.30$  ( $0.08 \leq m/M_{\odot} < 0.50$ ),  $\alpha_2 = +2.35$  ( $0.50 \leq m/M_{\odot} < 1.00$ ) and  $\alpha_3 = +2.35$  ( $1.00 \leq m/M_{\odot} < 150.00$ ), ie. Salpeter (1955) above  $0.5 M_{\odot}$ . A steeper value  $\alpha_3 = 2.7$  has been suggested by Kroupa et al. (1993) based on Scalo’s (1986) star-count analysis of the relatively local Galactic field. Such a steep IMF above  $1 M_{\odot}$  may be the correct IMF resulting from star-cluster formation if corrections for unresolved multiples among massive stars are applied (Sagar & Richtler 1991; Malkov & Zinnecker 2001). Alternatively, the Scalo value may reflect a steeper IGIMF (Kroupa & Weidner 2003). We use both, the canonical Salpeter  $\alpha_3$  and the Scalo value.

The cluster mass in stars is

$$M_{\text{ecl}} = \int_{m_{\text{low}}}^{m_{\text{max}}} m \cdot \xi(m) dm, \quad (3)$$

where  $m_{\text{low}} = 0.01 M_{\odot}$  is the adopted minimum mass given by opacity-limited fragmentation while  $m_{\text{max}}$  is the maximum stellar mass that can occur in the cluster. Apart from not well

understood physical reasons (Weidner & Kroupa 2004), it cannot be arbitrarily high because the cluster mass sets limits on its value. These can be formulated through conditional statistics. Statistically, a cluster with mass  $M_{\text{ecl}}$  contains exactly one most massive star,

$$1 = \int_{m_{\text{max}}}^{m_{\text{max}^*}} \xi(m) dm, \quad (4)$$

The resulting equation,  $m_{\text{max}}(M_{\text{ecl}})$ , cannot be solved analytically. Weidner & Kroupa (2004) solve it numerically and show that an upper bound on  $m_{\text{max}} \leq m_{\text{max}^*} \approx 150 M_{\odot}$  must exist as otherwise there would be too many stars with masses larger than about  $100 M_{\odot}$  in the LMC star-burst cluster R136. Weidner & Kroupa (2004) interpret  $m_{\text{max}^*}$  to be a fundamental upper stellar mass. Intriguingly, the same stellar mass limit is noted by Figer (2005) for the metal-rich MW-nuclear cluster Arches suggesting that perhaps  $m_{\text{max}^*} \approx 150 M_{\odot}$  may be quite independent of metallicity, and Oey & Clarke (2005) find such an upper mass limit based on statistical examinations of several clusters. Numerical simulations of star-formation in clusters (Bonnell et al. 2004) also indicate that the mass of the most massive star scales with the system (cluster) mass and is not a purely random value but a conditional one.

### 2.3. The integrated galaxial initial mass function

Under the assumption of an invariant canonical stellar IMF in clusters and an invariant ECMF (§ 1), the integrated galaxial initial mass function (IGIMF) is calculated by adding all stars in all clusters (as already noted by Vanbeveren 1982, 1983),

$$\xi_{\text{IGIMF}}(m, t) = \int_{M_{\text{ecl},\text{min}}}^{M_{\text{ecl},\text{max}}(SFR(t))} \xi(m \leq m_{\text{max}}) \xi_{\text{ecl}}(M_{\text{ecl}}) dM_{\text{ecl}}. \quad (5)$$

Thus  $\xi(m \leq m_{\text{max}}) \xi_{\text{ecl}}(M_{\text{ecl}}) dM_{\text{ecl}}$  is the stellar IMF contributed by  $\xi_{\text{ecl}} dM_{\text{ecl}}$  clusters with mass near  $M_{\text{ecl}}$ . While  $M_{\text{ecl},\text{max}}$  follows from eq. 1,  $M_{\text{ecl},\text{min}} = 5 M_{\odot}$  is adopted. The stellar mass in an embedded cluster is  $M_{\text{ecl}}$  so that the mass in stars and gas of the whole embedded cluster amounts to  $M_{\text{ecl}}/\epsilon$  for a star formation efficiency of  $\epsilon$  ( $\approx 1/3$ , Lada & Lada 2003). Note that in Kroupa & Weidner (2003) we referred to eq. 5 as the “field-star IMF”,  $\xi_{\text{field}}$ . This is strictly speaking not correct, because the IGIMF includes all stars in all clusters *and* the galactic field which consists of already dispersed clusters. However, as long as the surviving and newly-born star-clusters do not constitute a significant stellar contribution to the whole galaxy and ignoring issues arising from a flux limit,  $\xi_{\text{IGIMF}} \approx \xi_{\text{field}}$  for the time-averaged galaxy. Another way of looking at eq. 5 is to consider joint probabilities: The joint probability for finding a star of mass  $m$  in a cluster of mass  $M_{\text{ecl}}$  that has an upper stellar mass limit  $m_{\text{max}}$  is  $P(m, M_{\text{ecl}}) = P(m|M_{\text{ecl}}) \times P(M_{\text{ecl}})$ , where  $M_{\text{ecl}} = M_{\text{ecl}}(m_{\text{max}})$ .

Integrating over all cluster masses and scaling to the correct number of stars then recovers eq. 5.

The complete procedure is implemented in the following way: After the specification of a SFR for an individual star formation epoch the resulting  $M_{\text{ecl,max}}$  (eq. 1) is used to construct an ECMF with a predefined slope  $\beta$ . Each individual cluster in the ECMF is constructed from a predefined IMF up to a stellar mass limit determined by the mass of the individual cluster ( $m_{\text{max}}(M_{\text{ecl}})$ ). Then the separate IMFs of the clusters are added-up to give the IGIMF for this epoch (eq. 5). This is repeated with different SFRs to account for a varying SFH until the desired mass of the galaxy is reached at the desired age. The IGIMFs of the individual epochs are added to give the final IGIMF of the model galaxy.

It should be noted here that the IGIMF is not the PDMF as stellar evolution is not included, but it is the galaxy-wide IMF (galaxial IMF) which may be used to estimate certain properties of galaxies (as in § 3.1.2). The final IGIMF is, strictly speaking, only a theoretical construct because it counts all massive stars irrespective of when they are formed. To quantify the stellar population at any given moment we would need to include stellar evolution.

### 3. Results

Here we discuss the implications of our model for three different cases. In the first scenario (§ 3.1) so-called ‘standard’ parameters are used (stellar IMF slope above  $0.5 M_{\odot}$  being  $\alpha_2 = \alpha_3 = 2.35$ , and an ECMF slope  $\beta = 2.35$  for  $5 M_{\odot} \leq M_{\text{ecl}}$ , taking  $\beta = \alpha_3$  for simplicity). In § 3.2 we investigate a parameter set within the allowed range but which maximizes the effect on the IGIMF ( $\alpha_3 = 2.70$ ,  $\beta = 2.35$  for  $5 M_{\odot} \leq M_{\text{ecl}}$ ). Finally a set of parameters out of the allowed ones that minimize the effect is studied in § 3.3 ( $\alpha_3 = 2.35$  and a two-part power-law ECMF with  $\beta_1 = 1$  for  $5 \leq M_{\text{ecl}}/M_{\odot} \leq 50$ ,  $\beta_2 = 2$  for  $50M_{\odot} \leq M_{\text{ecl}}$ ), with some results also given for a ECMF truncated at  $50 M_{\odot}$  with  $\beta = 2$  for  $M_{\text{ecl}} \geq 50 M_{\odot}$ .

#### 3.1. The ‘standard’ scenario

##### 3.1.1. The IGIMF

*Panel A* of Fig. 2 shows the large differences of the final IGIMF for a galaxy with  $M_{\text{gal}} \lesssim 10^9 M_{\odot}$  in stars. Depending on the SFH such a galaxy can be a dwarf spheroidal

(dSph), a dwarf elliptical (dE), a dwarf irregular (dIrr) or a low-surface-brightness galaxy (LSB). We refer to such galaxies as “dwarf” galaxies. While in a single SF burst resulting in a dE system the IGIMF is populated up to the highest stellar masses, in the case of a LSB galaxy with a constant SFR the slope is much steeper and only stars up to  $\sim 25 M_\odot$  ever form. Low-mass LSB galaxies thus appear chemically very young.

Considering more massive galaxies ( $M_{\text{gal}} > 10^{10} M_\odot$  in stars, *panel B* of Fig. 2), the variation of the IGIMF with the SFR is not as pronounced as before. The weak dependence on the SFH comes about because even the continuous SFR is high enough to sample the ECMF to massive clusters such that the massive stars end up being well-represented. Note however that the resulting IGIMF is always significantly steeper than the canonical IMF, and equal to the canonical IMF below a few  $M_\odot$  (Kroupa & Weidner 2003).

The variation of the IGIMF is best illustrated by comparing the slope,  $\alpha_{\text{IGIMF}}$ , of the resulting IGIMFs (Fig. 3). In order to fit IGIMF slopes consistently the number of stars above  $m_{\text{knick}}$  (see Tab. 1) is calculated for each IGIMF up to the maximal mass of the corresponding model. This number,  $N_1$ , is compared with the corresponding number  $N_2$  calculated for a representative IGIMF with a single slope  $\alpha_{\text{IGIMF}}$  above  $m_{\text{knick}}$  up to the same mass limit. That  $\alpha_{\text{IGIMF}}$  is chosen to represent the IGIMF for which  $N_1 = N_2$ . Fig. 4 shows an example of the results of the automated fitting routine.

For dwarf galaxies a large difference is seen between models with continuous star formation (upper bound of the shaded area in Fig. 3) and a single, initial-burst of star formation (lower bound of the shaded area). All other SFHs would produce results in-between these two extremes.

Table 1: Down-turn (“knick”) masses for different model assumptions. For e.g.,  $m_{\text{knick}} = 1.307$  for the canonical models shown in Fig. 2.  $\beta_1$  and  $\beta_2$  are the power-law indices of the ECMF below and above  $50 M_\odot$ , respectively.

$\alpha_3$	$\beta_1$	$\beta_2$	$M_{\text{ecl,min}}$ [ $M_\odot$ ]	$m_{\text{knick}}$ [ $M_\odot$ ]
2.35	2.35	2.35	5	1.307
2.70	2.35	2.35	5	1.120
2.35	1.00	2.00	5	1.307
2.35	2.00	2.00	5	1.307
2.35	2.35	2.35	50	5.560
2.35	2.35	2.35	100	8.823

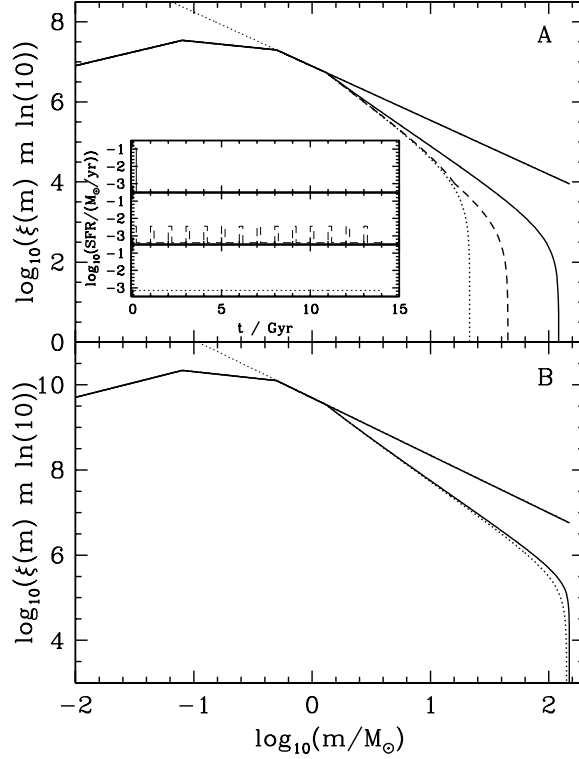


Fig. 2.— *Panel A*: IGIMFs for three galaxies with final stellar masses of  $10^7 M_{\odot}$  but different SFHs. The *solid curve* results from a single 100 Myr long burst of star formation. The *dashed curve* assumes a periodic SFH with 14 peaks each 100 Myr long and 900 Myr quiescent periods in between. The *thick dotted curve* assumes a constant SFR over 14 Gyr. For all cases the canonical IMF power-law slope above  $1 M_{\odot}$  ( $\alpha_3 = 2.35$ ) is used and the ECMF slope is  $\beta = 2.35$ . The *straight solid line* above  $0.5 M_{\odot}$  shows the canonical input IMF for comparison. The *thin dotted line* is a Salpeter IMF extended to low mass. Note the downturn of the IGIMFs at high masses. It results from the inclusion of a limiting maximum mass,  $m_{\max} \leq m_{\max*} = 150 M_{\odot}$ , into our formalism (Weidner & Kroupa 2004; Figer 2005). *Panel B*: As *panel A* but for a galaxy with  $10^{10} M_{\odot}$  in stars. The IGIMF is only shown for an initial-burst SFH (*solid curve*), giving an E-type galaxy, and for a continuous SFH (*dotted curve*) giving a MW-type galaxy.

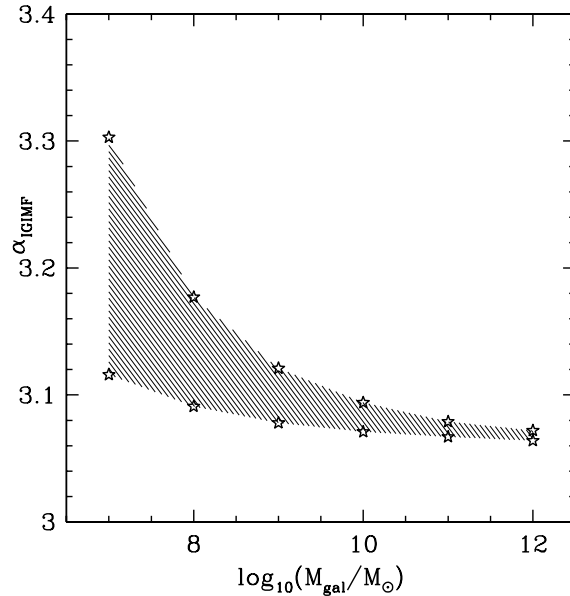


Fig. 3.— The resulting IGIMF slopes above  $m_{\text{knick}} = 1.3 M_{\odot}$  are shown in dependence of stellar galaxy mass for different models, as indicated. The lower bound of the shaded area is for an initial SF burst forming the entire stellar galaxy while the upper bound is derived for a continuous SFH. The symbols correspond to calculated models. The region within the shaded area corresponds to models with prolonged and time-varying SFHs. Note that we classify galaxies with  $M_{\text{gal}} \leq 10^9 M_{\odot}$  as dwarfs. These include dSph, dE, dIrr and LSB galaxies. A Salpeter IMF has  $\alpha = 2.35$ .

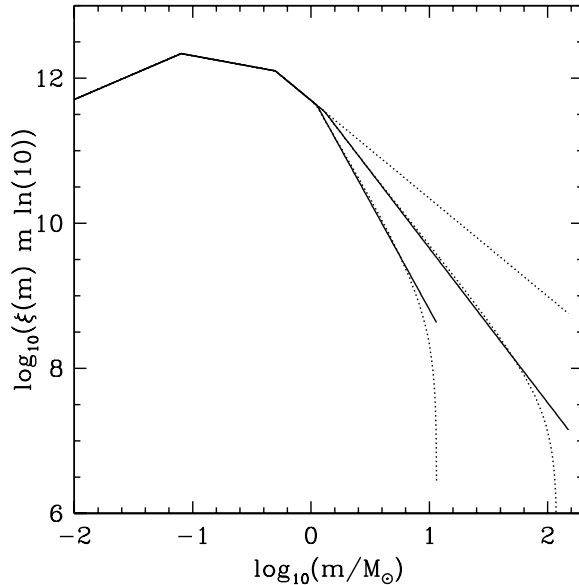


Fig. 4.— Two examples of how  $\alpha_{\text{IGMF}}$  is fitted. The straight dotted line is the canonical IMF (with  $\alpha_3 = 2.35$ ) while the other dotted lines are resulting IGIMFs for two models with  $M_{\text{gal}} = 10^7 M_{\odot}$ . The left one has an input  $\alpha_3 = 2.70$  and continuous star-formation over 14 Gyr and the right one an input  $\alpha_3 = 2.35$  and is formed in a single 100 Myr burst of star-formation. In both cases the ECMF has a slope of  $\beta = 2.35$ . The solid lines show the fits derived from our algorithm based on the assumption that the number of stars beyond  $m_{\text{knick}}$  is equal for the corresponding solid and dotted lines.

### 3.1.2. Number of supernovae of type II

The steeper IGIMF slopes imply a less-frequent occurrence of type II supernovae (SN) in galaxies. To quantify this we calculate from the IGIMFs of each galaxy model the total number of stars formed above  $8 M_{\odot}$  over a period of 14 Gyr. We then divide this number by the total number of stars in the galaxy in order to get the number of SN per star,  $\text{NSNS}_{\text{IG}}$  (integrated galaxial NSNS). The  $\text{NSNS}_{\text{IG}}$  is then divided by the NSNS for models in which the same mass in stars is distributed according to the canonical IMF ( $\alpha_3 = 2.35$  for  $m > 1.0 M_{\odot}$ ) to get the *relative NSNS for the IGIMF models in comparison to the NSNS expected from applying the (incorrect) canonical IMF* containing stars between 0.01 and  $150 M_{\odot}$ . For this (incorrect) model in which the stellar upper mass limit does not depend on the SFR, the  $\text{NSNS}_{\text{can}} = 0.003374$  SNII per star. Thus, we have

$$\text{NSNS}_{\text{IG}} = \frac{\int_8^{m_{\text{max}^*}} \xi_{\text{IGIMF}}(m) dm}{\int_{0.01}^{m_{\text{max}^*}} \xi_{\text{IGIMF}}(m) dm}, \quad (6)$$

and likewise for  $\text{NSNS}_{\text{can}}$  where  $\xi_{\text{IGIMF}}$  is replaced by  $\xi(m)$ . The relative NSNS is then given by,

$$\eta = \frac{\text{NSNS}_{\text{IG}}}{\text{NSNS}_{\text{can}}}. \quad (7)$$

The resulting  $\eta$  values are shown in Fig. 5 for  $\beta = 2$  and 2.35.

Two main effects are visible. Firstly the  $\eta$  are always smaller than for models with a constant canonical IMF ( $\eta < 1$ ). For example, for galaxies with a stellar mass of  $10^7 M_{\odot}$  the actual NSNS would be only 10 per cent of the NSNS expected traditionally by adopting a canonical IMF. Secondly, there is a strong dependence on galaxy mass:  $\eta$  decreases substantially with decreasing mass in stars.

The NSNS may thus be a strong function of the cosmological epoch, given that present-day galaxies are build-up from dwarfs through hierarchical merging.

Note that the traditional calculation based on an invariant Salpeter or canonical IMF leads to a constant NSNS independent of the SFR or galaxy mass. Often a Salpeter IMF is used for stars between 0.1 and  $100 M_{\odot}$ . Such an IMF has the constant  $\text{NSNS}_{\text{Salp}} = 0.002512$  which is 1.3 times smaller than the above constant  $\text{NSNS}_{\text{can}} = 0.003374$ .

## 3.2. The 'maximal' scenario

In this subsection we explore our so-called 'maximum' scenario where we adopt a slope of  $\alpha_3 = 2.7$  for the stellar IMF above  $1.0 M_{\odot}$ . Again we find that the effect is larger for

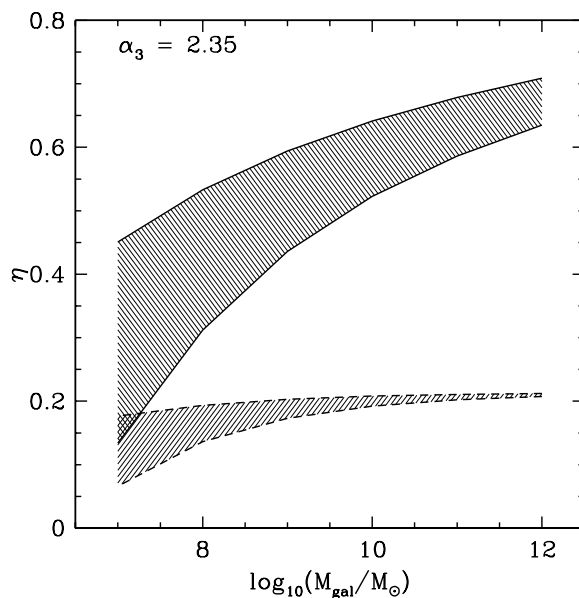


Fig. 5.— The relative NSNS in dependence of the stellar mass of the galaxy. The *upper shaded area* represents models with an ECMF slope  $\beta = 2$ , and for the *lower area*  $\beta = 2.35$ . The upper limit for each shaded region corresponds to a single-burst model while the lower limit is for continuous SF models. The (input) IMF slope for stars above  $1 M_{\odot}$  is  $\alpha_3 = 2.35$  (canonical) and the  $\eta$  plotted here are relative to the  $\text{NSNS}_{\text{can}}$  calculated for a constant canonical IMF (Salpeter above  $0.5 M_{\odot}$ ).

less-massive galaxies, and that the dependence of the IGIMF on the SFR is weak for massive galaxies. Fig. 6 illustrates the slopes of the IGIMF above  $m_{\text{knick}}$  in the maximal and the standard scenario introduced in § 3.1. Due to the steeper input slope all resulting slopes are shifted to larger values by about 0.5 dex and the spread between single initial-burst models and continuous SF models is somewhat larger for dwarf galaxies than in the standard scenario.

### 3.2.1. Number of supernovae of type II

The relative NSNS for the maximal scenario are shown in Fig. 7, again for two cases of the ECMF slope  $\beta$ . As expected  $\eta$  drops in comparison to the standard scenario (Fig. 5), and in the case of low-mass galaxies  $\eta$  can even become zero, meaning that there would be no SNII in such galaxies if the SFR is low enough.

## 3.3. Other ECMF and the ‘minimal’ scenario

In order to investigate the sensitivity of our results on a non-default ECMF at the lower mass end, three different assumptions for the ECMF are used: First by a flattening below  $50 M_{\odot}$  to a slope of  $\beta_1 = 1$  with  $\beta_2 = 2.35$  above  $50 M_{\odot}$ , and secondly by a lower-mass cut-off in the ECMF at  $50 M_{\odot}$  with  $\beta = 2.35$  above. As a result, the down-turn,  $m_{\text{knick}}$ , of the galaxial IMF is shifted to higher masses, but the deviations from the Salpeter value above  $1 M_{\odot}$  remain large. Finally we use a lower mass slope for the ECMF of  $\beta_1 = 1$  below  $50 M_{\odot}$  and additionally change the slope above to  $\beta_2 = 2$  in order to explore a minimal case. Due to the smaller  $\beta_2$  value of 2 in comparison with our other models the deviation from the canonical value is small in both panels of Fig. 8 for the initial-burst models and for massive galaxies in general. Never the less, for dwarf galaxies the difference between continuous SF and an initial-burst remains substantial.

### 3.3.1. Number of supernovae of type II

In Fig. 9  $\eta$  is shown for a flat ( $\beta_1 = 1$ ) ECMF below  $50 M_{\odot}$  (*panel A*) and for a cut-off below  $50 M_{\odot}$  (*panel B*). While in the first case  $\eta$  is still very low (20 to 40% of the corresponding canonical value), in the second case  $\eta$  increases up to 60% thus reducing the effect. In Fig. 10 is  $\eta$  shown for the minimal model with an ECMF slope of  $\beta_1 = 1$  below  $50 M_{\odot}$  and  $\beta_2 = 2$  above  $50 M_{\odot}$ . Here the deviations from the invariant canonical model

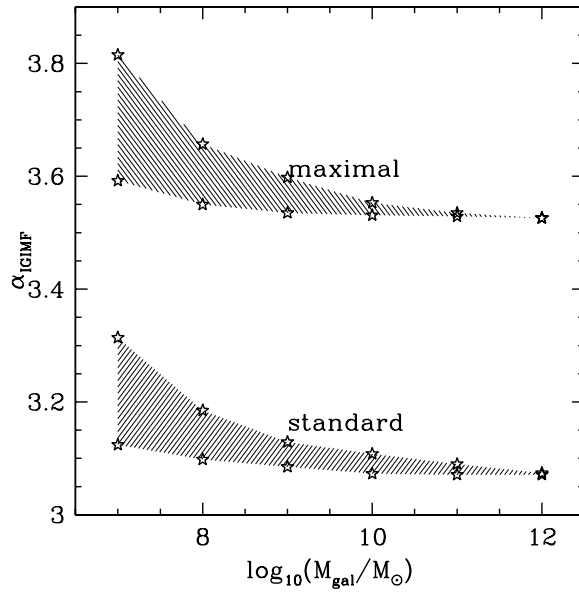


Fig. 6.— As Fig. 3 but with  $\alpha_3 = 2.70$ . The results of the 'standard' scenario with  $\alpha_3 = 2.35$  are the lower hatched region.

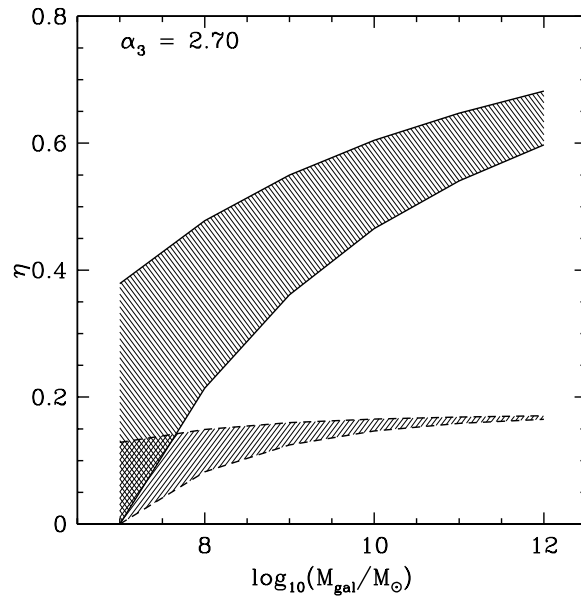


Fig. 7.— Like Fig. 5 but with an (input) IMF slope of  $\alpha_3 = 2.70$  for stars above  $1 M_{\odot}$ .

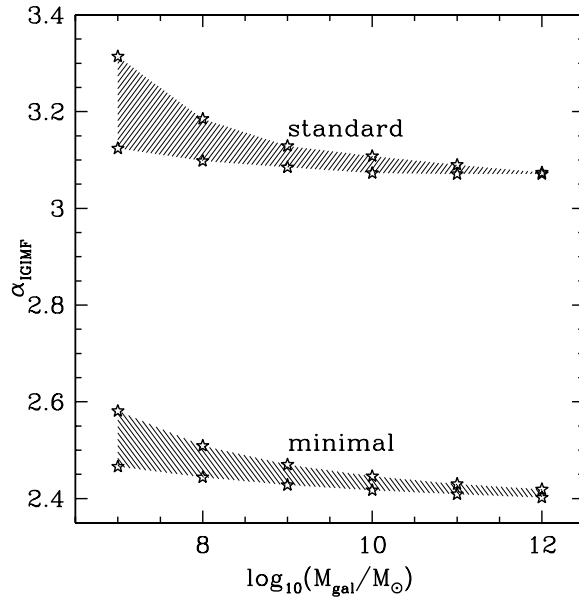


Fig. 8.— As Fig. 3 but with a 2-part-power-law ECMF with  $\beta_1 = 1.00$  and  $\beta_2 = 2.00$  and  $\alpha_3 = 2.35$ . The results of the 'standard' scenario are the upper hatched region with  $\beta = 2.35$  and  $\alpha_3 = 2.35$ .

are only about 20% for massive galaxies but are still about 50% for dwarf galaxies. Thus we find that even for assumptions that minimize the effects due to clustered star formation,  $\eta < 0.8$  for all galaxies, with smaller values for less-massive galaxies.

### 3.4. Comparison of the scenarios

For the efficient construction of models (IGIMF vs SFH) and for a useful comparison with observations we also compute the upper stellar mass limit and the IGIMF slope as functions of the galaxial SFR per epoch of 10 Myr duration (§ 2.1) for all three scenarios. The results are presented in Fig. 11. The upper mass limits (*panel A* of Fig. 11) are equal for the minimal and the standard scenario. The slopes of the IGIMF (*panel B* of Fig. 11) span a large range between the different scenarios, but in all cases steeper slopes are to be expected for low SFRs. The data plotted in Fig. 11 allow the construction of IGIMFs without the need to perform the detailed modelling described in this paper.

It is important to note here that the SFRs in Fig. 11 are not the averaged SFRs of the galaxy but the SFRs during the star-formation epoch. Thus, for example, a galaxy with  $M_{\text{gal}} = 10^7 M_{\odot}$  produced continuously over 1 Gyr has the same SFR of  $10^{-2} M_{\odot} \text{ yr}^{-1}$  and the same IGIMF and  $\eta$  as a galaxy with  $M_{\text{gal}} = 14 \times 10^7 M_{\odot}$  produced continuously over 14 Gyr. In order to get the complete stellar population of a galaxy the IGIMF slope of each star-formation epoch of the SFH has to be calculated, resulting in a series of populations, each with its own  $\xi_{\text{IGIMF}}(m, t)$ . These have to be added up to form the complete galaxy with the overall  $\xi_{\text{IGIMF}}$ .

## 4. Conclusions and Discussion

We show that it is possible to explain varying stellar populations in galaxies by a simple mechanism based on universal principles for all galaxies. Our assumptions are (i) that all stars are born in clusters following a universal embedded cluster mass function which is populated up to a maximum cluster mass which depends on the star formation rate of a galaxy, and (ii) that within these clusters all stars are born from a universal stellar IMF. But the magnitude of the effect strongly depends on the shape of the ECMF for low-mass clusters. The combination of a varying SFR with the empirical  $M_{\text{ecl,max}}(\text{SFR})$  relation, together with the stellar mass being limited by the cluster mass, naturally leads to a time-dependent integrated galaxial initial stellar mass function. This IGIMF also depends on the mass of the galaxy by virtue of the average level of the SFR being proportional to  $M_{\text{gal}}$ . The

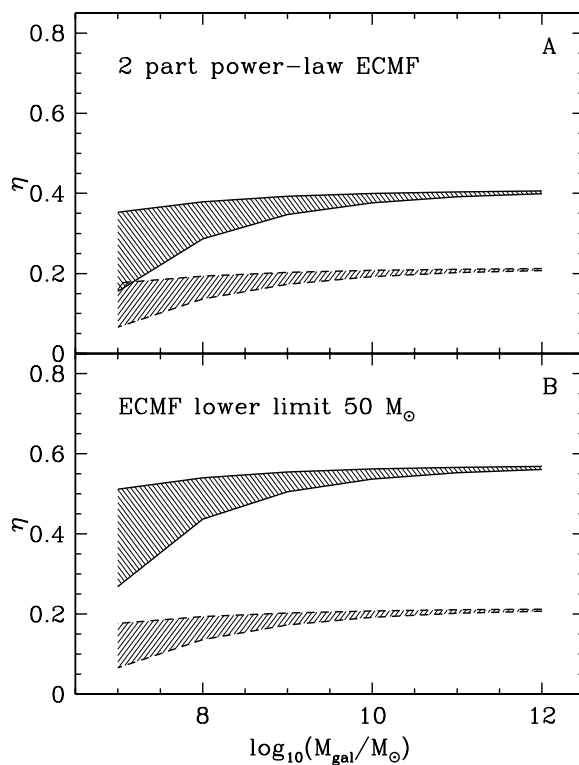


Fig. 9.— *Panel A*: Like Fig. 5 but with a flattening to  $\beta_1 = 1$  of the ECMF below  $50 M_\odot$ . *Panel B*: Like *panel A* but with  $M_{\text{ecl},\text{min}} = 50 M_\odot$  for the ECMF. In both cases  $\beta_2 = 2.35$  for  $M_{\text{ecl}} > 50 M_\odot$  and the shaded area enclosed by the *dashed curves* are the standard values from Fig. 5 (for  $\alpha_3 = 2.35$  and  $\beta = 2.35$ ).

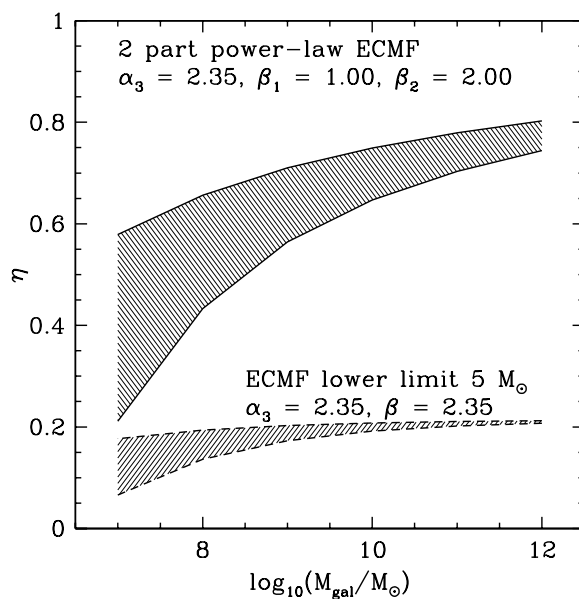


Fig. 10.— The minimal scenario, like Fig. 5 but with an ECMF slope  $\beta_1 = 1$  below  $50 M_\odot$  and  $\beta_2 = 2$  for  $M_{\text{ecl}} > 50 M_\odot$ . The shaded area enclosed by the *dashed curves* are the standard values from Fig. 5 (for  $\alpha_3 = 2.35$  and  $\beta = 2.35$ ).

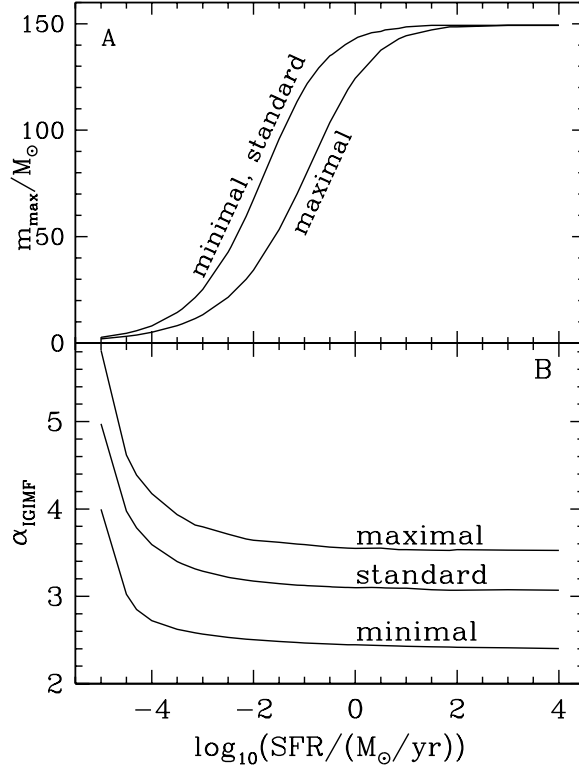


Fig. 11.— *Panel A:* The upper stellar mass limit ( $m_{\text{max}} \leq m_{\text{max},*} = 150 M_{\odot}$ ) as a function of the SFR of a galaxy per epoch of 10 Myr duration for the three scenarios. While for SFRs above  $1 M_{\odot} \text{yr}^{-1}$  the IMF is sampled up to the maximum stellar mass limit of about  $150 M_{\odot}$  (for details see Weidner & Kroupa 2004), the limit declines for lower SFRs. *Panel B:* The slope of the IGIMF generated during a star-formation epoch as a function of the SFR during that epoch.

steep IGIMF and the variations – especially for dwarf galaxies – may have implications for the chemo-dynamical evolution of galaxies. But we note that this effect occurs in addition to standard (i.e. IMF-invariant) variations of the relative number of young and old populations as a result of varying SFRs, making the empirical detection of IGIMF variations challenging. We document in Fig. 11 all quantities needed to construct, without additional computation, IGIMFs for galaxies of all morphological types and for a standard, a maximal and a minimal scenario. This ought to be useful for future chemo-dynamical research within a hierarchical cosmological structure formation scenario.

In summary, given our assumptions the most important conclusions are:

- Chemical enrichment histories and SN rates calculated with an invariant Salpeter IMF may not be correct for any galaxy;
- The number of supernovae is lower, and possibly significantly lower over cosmological times than for an invariant canonical IMF;
- Irrespective of how old a galaxy is it will always appear less chemically evolved than a more massive equally-old galaxy as a result of the steeper IGIMF;
- The scatter in chemical properties must increase with decreasing galaxy mass;
- A steeper (input) IMF above  $1 M_{\odot}$  would aggravate the systematic differences in galaxy properties when compared to a Salpeter IMF as well as increasing the variations with galaxy mass;

where galaxy mass refers only to the assembled mass in stars.

Of future interest would be a direct observational test of this model. This may be possible by using deep luminosity functions of nearby galaxies. But these functions will reflect the PDMF so that stellar evolution and the SFH need to be taken into account in order to extract the IGIMF. The difficulty associated with such work is seen by several studies of starburst galaxies having found (IG)IMFs truncated at the lower mass end near a few  $M_{\odot}$  (e.g. Wright et al. 1988), but more recent studies (Elmegreen 2004b; Gouliermis et al. 2004b, and references therein) showed that this seems not to be the case. In the same paper Elmegreen points out that a Salpeter IMF with a flattening below about  $0.5 - 1 M_{\odot}$  gives a good approximation for starburst galaxies. This does not necessarily contradict our result of a variable galaxy-wide IGIMF, as the observable part of the IGIMF in a starburst galaxy is dominated by a few young and massive clusters for which we adopt a Salpeter IMF in the high mass range. In our model variations come from the fainter less-massive clusters.

It should be noted here that for the more conservative approach of the minimal scenario our results still predict considerable differences in comparison with a constant canonical IMF. For example, Goodwin & Pagel (2004) make assumptions rather similar to our minimal scenario and predict a reduction of the general metal yield by a factor of about 1.8.

### Acknowledgments

We thank John Scalo for very useful suggestions. This work has been funded by DFG grant KR1635/3.

### REFERENCES

- Adams, F. C., & Myers, P. C. 2001, *ApJ*, 553, 744
- Alonso-Herreó, A., Rieke, G. H., Rieke, M. J., & Scoville, N. Z. 2002, *AJ*, 124, 166
- Bell, E. F., McIntosh, D. H., Katz, N., & Weinberg M. D. 2003, *ApJS*, 149, 289
- Blitz, L., & Rosolowski, E. 2004, to appear in "IMF@50: The Initial Mass Function 50 Years Later", ed. E. Corbelli, F. Palla, & H. Zinnecker (Dordrecht: Kluwer), in press (astro-ph/0411520)
- Bonnell, I. A., Vine, S. G., & Bate, M. R. 2004, *MNRAS*, 349, 735
- Brandl, B., Sams, B. J., Bertoldi, F., Eckart, A., Genzel, R., Drapatz, S., Hofmann, R., Loewe, M., & Quirrenbach, A. 1996, *ApJ*, 466, 254
- Cresci, G., Vanzi, L., & Sauvage, M. 2004, *A&A*, in press (astro-ph/0411486)
- de Grijs, R., Gilmore, G. F., Johnson, R. A., & Mackey, A. D. 2002, *MNRAS*, 331, 245
- de la Fuente Marcos, R., & de la Fuente Marcos, C. 2004, *New Astron.*, 9, 475
- de Marchi, G., Paresce, F., & Portegies Zwart, S. 2004, to appear in "IMF@50: The Initial Mass Function 50 Years Later", ed. E. Corbelli, F. Palla, & H. Zinnecker (Dordrecht: Kluwer), in press (astro-ph/0409601)
- Elmegreen, B. 1999, *ApJ*, 515, 323
- Elmegreen, B. 2004a, *MNRAS*, 354, 367

- Elmegreen, B. 2004b, to be appear in "Starbursts: from 30 Doradus to Lyman Break Galaxies," ed. de Grijs, R., & Gonzalez Delgado, R. M. (Dordrecht: Kluwer), in press (astro-ph/0411193)
- Figer, D. 2005, in preparation
- Goodwin, S. P., Pagel, B. E. J. 2004, submitted to MNRAS (astro-ph/0410068)
- Gouliermis, D., Keller, S. C., Kontizas, M., Kontizas E., & Bellas-Velidis, I. 2004a, A&A, 416, 137
- Gouliermis, D., Brandner, W., & Henning, Th. 2004b, ApJ, in press (astro-ph/0411448)
- Gualandris, A., Portegies Zwart, S., & Eggleton, P. P. 2004, MNRAS, 350, 615
- Hunter, D. A., Elmegreen, B. G., Dupuy, T. J., & Mortonson, M. 2003, AJ, 126, 1836
- Kalirai, J. S., Fahlman, G. G., Richer, H. B., & Ventura, P. 2003, AJ, 126, 1402
- Kennicutt, R. C. Jr., Edgar, B. K., & Hodge, P. W. 1989, ApJ, 337, 761
- Kroupa, P. 2001, MNRAS, 322, 231
- Kroupa, P. 2002, Science, 295, 82
- Kroupa, P. 2004, to appear in the Proceedings of the Symposium "The Three-Dimensional Universe with Gaia", ed. Turon, C., O'Flaherty, K. S., Perryman, M. A. C. (ESA SP-576), in press (astro-ph/0412069)
- Kroupa, P., & Boily, C. M. 2002, MNRAS, 336, 1188
- Kroupa, P., & Bouvier, J. 2003, MNRAS, 346, 343
- Kroupa, P., & Weidner, C. 2003, ApJ, 598, 1076
- Kroupa, P., Aarseth, S., & Hurley, J. 2001, MNRAS, 321, 699
- Kroupa P., Tout C. A., & Gilmore G. 1993, MNRAS, 262, 545
- Lada, C. J., & Lada, E. A. 2003, ARA&A, 41, 57
- Malkov, O., & Zinnecker, H. 2001, MNRAS, 321, 149
- Massey, P. 2002, ApJS, 141, 81
- Massey, P. 2003, ARA&A, 41, 15

- Massey, P., & Hunter, D. A. 1998, *ApJ*, 493, 180
- McCrary, N., Graham, J. R., & Vacca, W. D. 2004, *ApJ*, in press (astro-ph/0411256)
- Moraux, E., Kroupa, P., & Bouvier, J. 2004, *A&A*, 426, 75
- Oey M. S., Clarke C. J., 2005, *ApJL*, in press (astro-ph/0501135)
- Parker, J. W., Zaritsky, D., Stecher, T. P., Harris, J., & Massey, P. 2001, *AJ*, 121, 891
- Piskunov, A. E., Belikov, A. N., Kharchenko, N. V., Sagar, R., & Subramaniam, A. 2004, *MNRAS*, 349, 1449
- Prisinzano, L., Carraro, G., Piotto, G., Seleznev, A. F., Stetson, P. B., & Saviane, I. 2001, *A&A*, 369, 851
- Prisinzano, L., Micela, G., Sciortino, S., & Favata, F. 2003, *A&A*, 404, 927
- Reid I. N., Gizis J. E., & Hawley S. L. 2002, *AJ*, 124, 2721
- Sagar, R., & Richtler, T. 1991, *A&A*, 250, 324
- Sagar, R., Naidu, B. N., & Mohan, V. 2001, *BASI*, 29, 519
- Salpeter, E. E. 1955, *ApJ*, 121, 161
- Sanner, J., & Geffert, M. 2001, *A&A*, 370, 87
- Scalo, J. M. 1986, *Fundam. of Cosmic Phys.*, 11, 1
- Scalo, J. M. 1998, in Gilmore, G. & Howell, D., eds., *ASP Conf. Ser. Vol. 142, The Stellar Initial Mass Function*, 201
- Scalo, J. M. 2004, to appear in "IMF@50: The Initial Mass Function 50 Years Later", ed. E. Corbelli, F. Palla, & H. Zinnecker (Dordrecht: Kluwer), in press (astro-ph/0412543)
- Sirianni, M., Nota, A., De Marchi, G., Leitherer, C., & Clampin, M. 2000, *ApJ*, 533, 203
- Sirianni, M., Nota, A., De Marchi, G., Leitherer, C., & Clampin, M. 2002, *ApJ*, 579, 275
- Soares, J. B., Bica, E., Ahumada, A. V., & Clairá, J. J. 2004, *A&A*, in press (astro-ph/0411169)
- Thilker, D. A., Walterbros, R. A. M., Braun, R., & Hoopes, C. G. 2002, *AJ*, 124, 3118
- Vanbeveren, D. 1982, *A&A*, 115, 65

Vanbeveren, D. 1983, *A&A*, 124, 71

Weidner, C., & Kroupa, P. 2004, *MNRAS*, 348, 187

Weidner, C., Kroupa, P., & Larsen, S. S. 2004, *MNRAS*, 350, 1503

Wright, G. S., Joseph, R. D., Robertson, N. A., James, P. A., & Meikle, W. P. S. 1988, *MNRAS*, 233, 1

Wyse, R. F. G., Gilmore, G., Houdashelt, M. L., Feltzing, S., Hebb, L., Gallagher, J. S., III, & Smecker-Hane, T. A. 2002, *New Astron.*, 7, 395

Youngblood, A. J., & Hunter, D. A. 1999, *ApJ*, 519, 55

Zhang, Q., & Fall, S. M. 1999, *ApJL*, 527, L81